Polymer Grafting onto Starch Nanocrystals

Marianne Labet,† Wim Thielemans,† and Alain Dufresne*

Ecole Française de Papeterie et des Industries Graphiques de Grenoble, Institut National Polytechnique de Grenoble, BP 65, 38402 Saint Martin d'Hères Cedex, France

Received April 27, 2007; Revised Manuscript Received July 3, 2007

Monocrystalline starch nanoparticles were successfully grafted with poly(tetrahydrofuran), poly(caprolactone), and poly(ethylene glycol) monobutyl ether chains using toluene 2,4-diisocyanate as a linking agent. Surface grafting was confirmed using Fourier transform infrared and X-ray photoelectron spectroscopies, differential scanning calorimetry, elemental analysis, and contact angle measurements. Transmission electron microscopy observations of modified starch nanocrystals showed either the individualization of nanoparticles or the formation of a film, depending on the polymer used. It was shown that grafting efficiency decreased with the length of the polymeric chains, as expected. The resulting modified nanoparticles can find applications in the field of co-continuous nanocomposite materials.

Introduction

Current society produces more and more waste. A large amount of this waste arises from packaging, and it is generally not biodegradable as these materials involve complex composites and are petroleum-based.[1] Moreover, there is a huge interest in the processing of packaging materials filled with nanoscale components. These nanocomposites present a higher interface in comparison to traditional microscale composites. Therefore, there is a growing interest for bio-nanocomposites, i.e., nanocomposites for which at least one, or preferably both, of the components are derived from renewable resources.

Polysaccharides, such as starch, cellulose, and chitin, are interesting renewable resources for nonfood applications. Indeed, as they are obtained from biomass, they are available in large quantities, renewable, and biodegradable and have a low cost. Among polysaccharides, starch is probably the most promising material for packaging. It is the cheapest biopolymer, and it is totally biodegradable. The usual way to process films from starch consists of converting it into a thermoplastic polymer by mixing with enough water or a nonaqueous plasticizer (generally polyols). The resulting material can be manufactured using technology already developed for the production of synthetic plastics, thus representing a minor investment. However, the hydrophilic nature of plasticized starch makes it susceptible to moisture attack, resulting in changes in dimensional stability and mechanical properties. In addition, retrogradation and crystallization of the mobile starch chains lead to an undesired change in mechanical and thermomechanical properties.

During the last 10 years, polysaccharides, mainly cellulose, have been used to prepare nano-reinforcements that can be used to prepare nanocomposite materials.[2,3] In particular, it has been known for a long time how to obtain nanocrystals from starch, by carrying out an acid hydrolysis on starch native granules.[4,5] The detailed morphological characterization of platelet-like nanoparticles obtained by acid hydrolysis of starch granules was reported.[6] They consist of crystalline nanoplatelets about 6−8 nm thick with a length of 20−40 nm and a width of 15−30 nm. A previous work consisted of optimizing the preparation of nanocrystals from waxy maize granules.[7] Optimized conditions have been stated using sulfuric acid. These starch nanocrystals displayed interesting reinforcing properties when dispersed in poly(styrene-*co*-butyl acrylate)[8,9] or natural rubber.[10−12] Interesting reinforcing capability was also obtained for nanocrystals of reinforced starch plasticized by glycerol.[13] In addition, a considerable slowing down of the recrystallization of the thermoplasticized starch matrix during storage in a humid atmosphere was reported. It resulted in a slower evolution of the mechanical properties of filled materials compared to the unfilled matrix. Sorbitol-plasticized pullulan films filled with waxy maize starch nanocrystals showed enhanced mechanical and water resistance properties.[14] All these composites were obtained by physically mixing the nanoparticles and the polymeric matrix.

The surface chemical modification of starch nanoparticles with short grafting agents was also reported.[15] However, the mechanical properties of nanocomposite materials processed from these modified nanocrystals and natural rubber were found to be lower than those for unmodified nanoparticles.[11] It was ascribed to the crucial role played by particle−particle interactions. Recently, we reported the grafting of larger chains on the surfaces of starch nanocrystals.[16] In this previous work, medium-chain-length stearic acid chloride and poly(ethylene glycol) methyl ether were used. The described surface modifications had a layer thickness on the order of magnitude of the thickness of starch nanoparticles. However, the length of the grafted chains was not sufficient to allow the formation of a continuous film by hot-pressing the modified nanoparticles.

The present work is a continuation of previous work by Thielemans et al.[16] We chose poly(tetrahydrofuran) (PTHF), poly(propylene glycol) monobutyl ether (PPGBE), and poly(caprolactone) (PCL). PPGBE was chosen for the good compatibility of starch with poly(propylene glycol) and its applicability to drug and other medical products, whereas PCL was chosen because of its biodegradability. PTHF falls in between these two polymers. The described surface modifications have an expected layer thickness ranging between 0.5 and 20 times the

* Author to whom correspondence should be addressed. E-mail: Alain.Dufresne@efpg.inpg.fr.

† Present address: Driving Innovation in Chemistry and Chemical Engineering, School of Chemistry and School of Chemical, Environmental and Mining Engineering, The University of Nottingham, University Park, Nottingham NG7 2RD, United Kingdom.

10.1021/bm700468f CCC: $37.00
Published on Web 08/24/2007

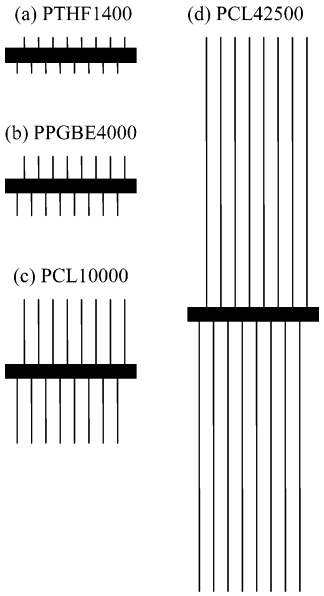

Figure 1. Relative sizes of the grafted stretched chains for (a) PTHF1400, (b) PPGBE4000, (c) PCL10000, and (d) PCL42500 in comparison to the thickness of starch nanocrystals.

thickness of starch nanoparticles when considering stretched polymeric chains. These chain lengths were expected to be high enough to allow the formation of a continuous film by hot-pressing the modified nanoparticles.

Experimental Section

Materials. Amylopectin-rich waxy maize starch (trade name Waxylis 200) was obtained from Roquette S.A. (Lestrem, France) and used as received. Sulfuric acid (≥95%), toluene 2,4-diisocyanate (2,4-TDI, 95%), phenylisocyanate (PhNCO), triethylamine (99.5%), diiodomethane, *N*,*N*-dimethyl formamide (NN-DMF), poly(tetrahydrofuran) (M_n = 1400 g mol^{-1}), poly(propylene glycol) monobutyl ether (M_n = 4000 g mol^{-1}), and poly(caprolactone) (M_n = 10 000 g mol^{-1} and M_n = 42 500 g mol^{-1}) were obtained from Sigma-Aldrich. Acetone and dichloromethane were obtained from Chimie-Plus Laboratoires. Potassium bromide was obtained from Acros Organics. Toluene was dried over molecular sieves. Polymers were dried in a desiccator for 1 week over P_2O_5.

Four polymers were grafted onto the starch residues. The schematic representation in Figure 1 gives an idea of the grafted chain length considering it as fully extended compared to the starch nanocrystal thickness.

(i) Poly(tetrahydrofuran) (M_n = 1400 g mol^{-1}) has the chemical structure that is presented in Scheme 1a. Considering the length of the stretched chain, this polymer is 4.2 nm long, corresponding to about 70% of the starch nanocrystals thickness (Figure 1a).

(ii) Poly(propylene glycol) monobutyl ether (M_n = 4000 g mol^{-1}), whose chemical structure is presented in Scheme 1b, is 9.1 nm long in its fully stretched state, or about 150% of the starch nanocrystals thickness (Figure 1b).

(iii) Poly(caprolactone) (M_n = 10 000 g mol^{-1}, M_w = 14 000 g mol^{-1}) has the chemical structure that is presented in Scheme 1c. Considering the length of the stretched chain, this polymer is 26.7 nm long, which is about 445% of the starch nanocrystal thickness (Figure 1c).

(iv) Poly(caprolactone) (M_n = 42 500 g mol^{-1}, M_w = 65 000 g mol^{-1}) has the chemical structure presented in Scheme 1d. The stretched chain length is 113.1 nm long or 1885% of the starch nanocrystal thickness (Figure 1d).

Starch Nanocrystal Preparation. Starch nanocrystals were prepared by acid hydrolysis of waxy maize starch granules for 5 days at 40 °C

Scheme 1. Chemical Structures of (a) PTHF1400, (b) PPGBE4000, (c) PCL10000, and (d) PCL42500

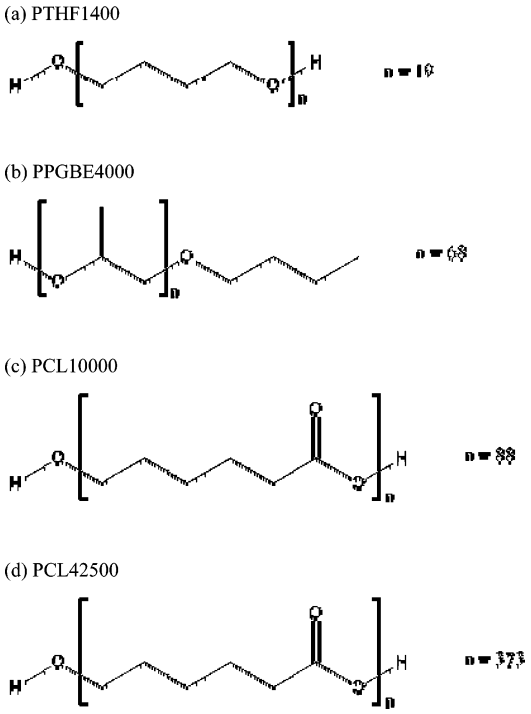

in a 3.16 M aqueous H_2SO_4 solution while stirring constantly, as described in detail and optimized elsewhere.[7] The resulting suspension was then washed with distilled water by successive centrifugations at 10 000 rpm and 10 °C for 20 min until the pH of the suspension was neutral. Then solvent exchange was done from distilled water to acetone, then from acetone to toluene by successive centrifugations at 10 000 rpm and 10 °C for 45 min (three centrifugations for each solvent). A homogeneous dispersion of starch nanocrystals in toluene was obtained by using an Ultra Turrax T25 homogenizer for 3 min at 13 500 rpm. Complete hydrolysis was confirmed by transmission electron microscopy and by agreement of the final product yield with earlier results.[7]

Surface Grafting Reactions. Chemical modification of the starch nanoparticles was performed in a round-bottomed reaction flask under a nitrogen atmosphere while constantly stirring with a magnetic stir bar. Reactant amounts and reaction time and temperature are reported in Table 1. Not only the amount but also the number of millimoles of each reagent (polymer, PhNCO, and 2,4-TDI) have been reported in Table 1. The density and molecular weight of PhNCO and 2,4-TDI necessary for the calculation were taken as 119.12 g mol^{-1} and 1.096 g cm^{-3} and 174.16 g mol^{-1} and 1.214 g cm^{-3}, respectively. The reaction schemes are shown in Scheme 2. All reactants and solvent (Table 1) were combined and left to react for 7 days. Triethylamine (TEA) was added to the reaction mixture to catalyze the reaction.

Poly(tetrahydrofuran) and poly(caprolactone) modifications involve a three-step process. The first step requires the reaction of phenylisocyanate with one functionality of the polymer. The molar ratios of PhNCO to polymer are 0.934, 2.79, and 1.52 for PTHF1400, PCL10000, and PCL42500, respectively. The second step requires the reaction of the modified polymer, having thus one protected functionality, with one isocyanate functionality of 2,4-TDI. For PPGBE4000, the first step is unnecessary, and the molar ratio of 2,4-TDI to polymer is 1.00. During the third step, the unreacted second isocyanate functionality of 2,4-TDI is then able to react with the surface hydroxyl groups of the starch nanoparticules to graft the polymer chain onto the nanoparticle. It has been shown that the isocyanate at the 4-position is 7 times more reactive than the isocyanate at the 2-position, such that the 4-position is expected to react first, in agreement with the literature.[17]

The polymer (PTHF or PCL) and toluene were placed into a three-necked round-bottomed flask equipped with a reflux condenser, kept

Table 1. Reaction Times and Temperatures and Reactant Amounts for (a) Function Protection, (b) Grafting Agent Synthesis, and (c) Starch Nanocrystal Modification

	PTHF1400 modification	PPGBE4000 modification	PCL10000 modification	PCL42500 modification
(a) Capping of the Second Hydroxyl Group on the Polymer Chain End				
solvent	108.64 mL		6980.40 mL	2473.50 mL
polymer	108.64 g/77.6 mmol		116.40 g/8.31 mmol	824.50 g/12.7 mmol
PhNCO	8.42 mL/72.5 mmol	no protection function	2.52 mL/23.2 mmol	2.10 mL/19.3 mmol
catalyst	2 mL		2 mL	3 mL
reaction temperature	70−80 °C		70−80 °C	70−80 °C
reaction time	4 h		4 h	4 h
(b) Grafting Agent Synthesis				
solvent (in addition to previous mixture)	100 mL	620.80 mL	200 mL	500 mL
polymer	previous mixture	310.40 g/77.6 mmol	previous mixture	previous mixture
2,4-TDI	11.16 mL/77.8 mmol	11.16 mL/77.8 mmol	3.34 mL/23.3 mmol	2.78 mL/19.4 mmol
catalyst		2 mL		
reaction temperature	70−80 °C	70−80 °C	70−80 °C	70−80 °C
reaction time	24 h	24 h	24 h	24 h
(c) Starch Nanocrystal Modification				
starch nanocrystals	2 g	2 g	2 g	2 g
polymer	previous mixture	previous mixture	previous mixture	previous mixture
reaction temperature	70−80 °C	70−80 °C	70−80 °C	70−80 °C
reaction time	7 days	7days	7 days	7 days

under a nitrogen atmosphere, and heated to the reaction temperature. The catalyst TEA was then added while stirring vigorously. PhNCO was subsequently added dropwise. The reaction was followed by Fourier transform infrared (FTIR) spectroscopy, and it was assumed to be complete after 4 h.

2,4-TDI was placed in a separate three-necked round-bottomed flask equipped with a reflux condenser and heated to the reaction temperature under a nitrogen atmosphere. Dropwise addition of the previous mixture (protected polymer, toluene, and catalyst) started the synthesis of the grafting agent. As isocyanate functions were in excess during the reaction, the isocyanate in the 4-position reacts preferentially. The reaction was followed by FTIR spectroscopy, and it was completed after 24 h.

Addition of starch nanocrystals in toluene to the previous mixture started the grafting reaction. This reaction was stopped after 7 days.

Grafting of PPGBE (M_n = 4000 g/mol) involved only a two-step process since no capping of a second hydroxyl functionality using PhNCO is necessary. The first step required the reaction of the polymer with the isocyanate at the 4-position of 2,4-TDI. During the second step, the unreacted second isocyanate functionality of 2,4-TDI was then reacted with the surface hydroxyl groups of the starch nanoparticules to graft the polymer chain onto the starch nanocrystals.

Toluene was placed into a three-necked round-bottomed flask equipped with a reflux condenser, kept under a nitrogen atmosphere, and heated to the reaction temperature. 2,4-TDI was added while vigorously stirring. The catalyst TEA was subsequently added. The reaction was started by the dropwise addition of polymer (PPGBE). Again, as isocyanate was in excess, the 4-position reacts preferentially. The reaction was followed by FTIR spectroscopy and found to be completed after 24 h.

Addition of starch nanocrystals in toluene to the previous reaction mixture started the grafting reaction. This grafting reaction was again stopped after 7 days.

After 7 days, each mixture (starch with PTHF, PPGBE, and PCL) was washed three times with toluene with successive centrifugations at 10 000 rpm and 10 °C for 45 min. It was then washed with dichloromethane again with three successive centrifugations in the same conditions to remove ungrafted polymer chains, any formed urea, isocyanates, and catalyst. The washed modified starch nanocrystals were subsequently Soxhlet extracted with dichloromethane for 24 h before drying at 50 °C in a convective oven.

It is worth noting that the end hydroxyl groups in PTHF should have similar reactivity, so in reaction I reported in Scheme 2a, although the molar ratio PhNCO/PHTF used was 1:1, a mixture of mono- and diurethane could have been formed. If this is the case, a part of PTHF will be inert in reaction II in Scheme 2a, and consequently a lower concentration of the grafting agent will be available for reaction III in Scheme 2a. This might explain the lower grafting efficiency that will be observed for PTHF. Concerning reaction I reported in Scheme 2b, it is also worth noting that the isocyanate group has a higher reactivity toward hydroxyl groups, so it might be expected that primarily the end hydroxyl group will react, but reaction with the carboxyl group might not be excluded. Therefore, also in this case a mixture of products is most probably obtained.

Characterization of the Grafted Starch Nanocrystals. FTIR spectroscopy was used to follow the reactions and to compare grafted to unmodified starch nanoparticles. FTIR spectrograms were recorded by the deposit of a drop of the reaction mixture between two NaCl windows, each hour after the beginning of the reaction. Four scans were taken between 4400 and 600 cm^{-1} with a 2 cm^{-1} interval. Comparison between grafted and unmodified starch nanocrystals was obtained by the inclusion of the dried powder in KBr pellets in a ratio of 99:1 KBr/starch. Sixty-four scans were taken between 4400 and 450 cm^{-1} with a 2 cm^{-1} interval. All FTIR spectrograms were obtained on a Perkin-Elmer Paragon 1000 FTIR spectrometer, and all spectra were analyzed using SpectrumNT software.

Transmission electron micrographs of either unmodified or grafted starch nanocrystals were taken with a Philips CM200 transmission electron microscope using an acceleration voltage of 80 kV. Transmission electron microscopy (TEM) was performed for modified starch nanocrystals deposited on a carbon-coated grid from a dispersion using a 2% uranyl acetate solution as a negative staining liquid.

Differential scanning calorimetry (DSC) was performed on a DSC Q100 (TA Instruments, New Castle, DE) fitted with a manual liquid nitrogen cooling system. Starch powder, conditioned at 0% relative humidity over P_2O_5 in a desiccator, was placed in a hermetically closed DSC crimp-sealed pan. Samples were tested in the range from −100 to 350 °C at a heating rate of 10 °C min^{-1} under a nitrogen atmosphere. The sample weight was between 2 and 5 mg.

Contact angle measurements were performed at room temperature using a dynamic drop tensiometer (ITConcept, Longessaine, France). The contact angle and drop volume were monitored as a function of time using WINDROP software. Three different liquids, with different dispersive and polar surface tensions, were used to determine the surface energy of the starch nanocrystals (Table 2). The drop volume was between 5 and 10 μL, and smooth surface starch samples were obtained

Scheme 2. Reaction Scheme for the Grafting of (a) PTHF, (b) PCL, and (c) PPGBE onto the Starch Nanocrystal Surface[a]

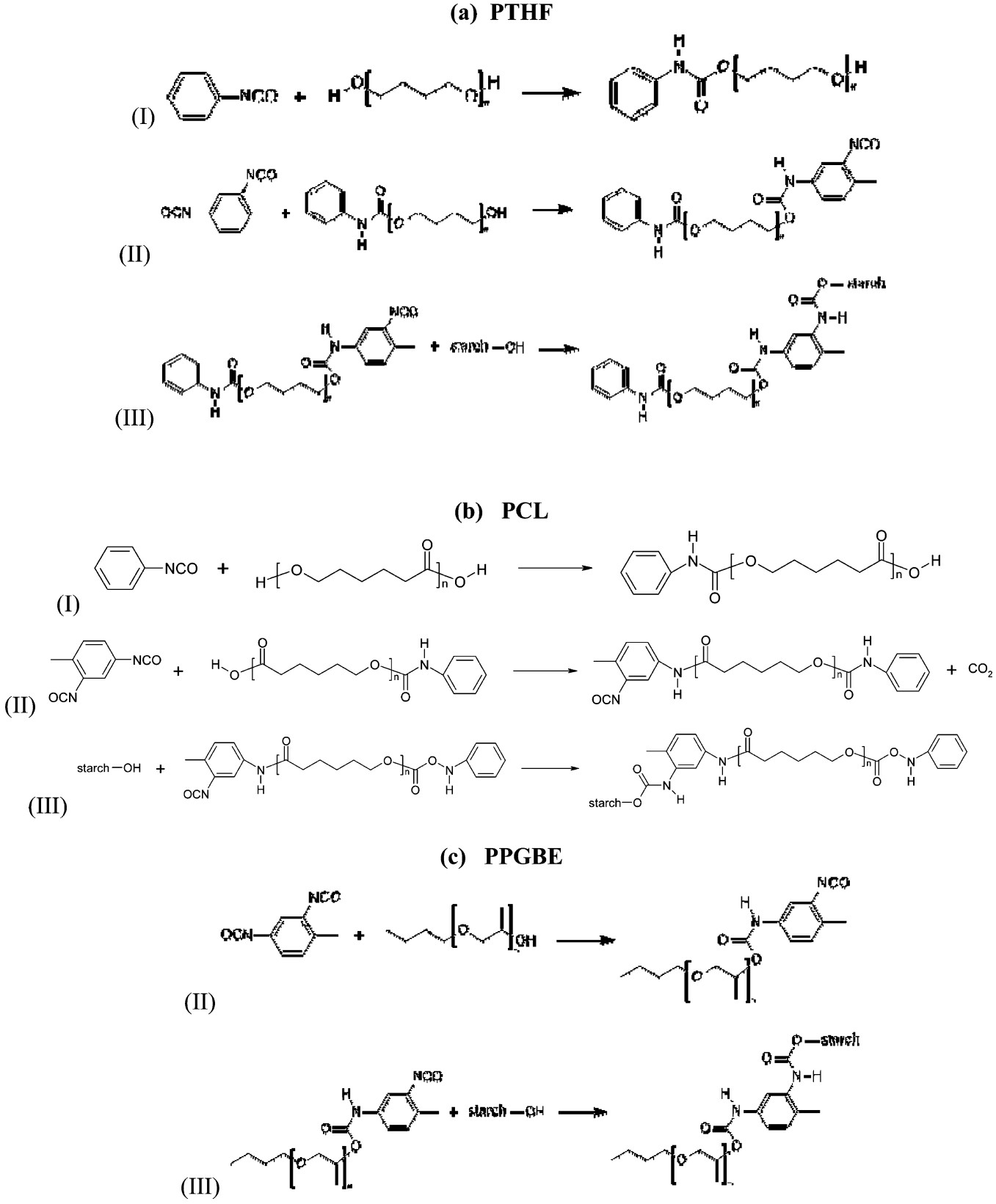

[a] (I) Capping of the second hydroxyl group on the polymer chain end, (II) reaction of the polymer chain with 2,4-TDI to give rise to the grafting agent, and (III) grafting of the starch nanocrystals.

by compacting the powder under a pressure of 10 metric tons using a KBr press. Contact angle measurements were carried out on starch nanocrystal samples before and after surface modification.

The Owens−Wendt approach was used to relate the dispersive and polar contributions to the surface energy of the starch samples to the dispersive and polar contributions of the surface tension of the liquids used and to their equilibrium contact angle with the starch surface (where the work of adhesion was replaced by the Young equation)[18]

$$\gamma_L(1 + \cos\theta) = 2\sqrt{\gamma_L^d \gamma_S^d} + 2\sqrt{\gamma_L^p \gamma_S^p} \quad (1)$$

Table 2. Surface Tension Contributions (Total, γ, Dispersive, γ^d, and Polar, γ^p, Surface Energy) for Liquids Used for Contact Angle Measurements

	water	diiodomethane	*N,N*-dimethyl formamide
γ (mN m^{-1})	72.8	50.8	58.0
γ^d (mN m^{-1})	21.8	49.5	39.0
γ^p (mN m^{-1})	51.0	01.3	19.0

with γ, γ^d, and γ^p being the total, dispersive, and polar surface energy, respectively. Subscripts L and S refer to the liquid drop and the solid surface, respectively, and θ denotes the contact angle between the solid substrate and the liquid drop. The liquid surface tensions were taken from the literature and are combined in Table 2.

According to eq 1

$$\frac{\gamma_L(1+\cos\theta)}{2\sqrt{\gamma_L^d}} = \sqrt{\gamma_S^d} + \sqrt{\frac{\gamma_L^p}{\gamma_L^d}}\sqrt{\gamma_S^p} \quad (2)$$

The left-hand side of eq 2 is a function of the known liquid surface tension contributions. From the linear relation

$$\frac{\gamma_L(1+\cos\theta)}{2\sqrt{\gamma_L^d}} = f\left(\sqrt{\frac{\gamma_L^p}{\gamma_L^d}}\right) \quad (3)$$

where $\sqrt{\gamma_S^p}$ and $\sqrt{\gamma_S^d}$ are the slope and the *y*-axis intercept, respectively, for each of the materials tested. The total surface energy of starch nanocrystals is easily obtained by the following equation

$$\gamma_S = \gamma_S^d + \gamma_S^p \quad (4)$$

Elemental Analysis was carried out by the Analysis Central Service of the Centre National de la Recherche Scientifique, Vernaison, France. The carbon, nitrogen, and oxygen contents of starch nanocrystals were measured independently.

X-ray photoelectron spectroscopy (XPS) experiments were carried out using an XR3E2 apparatus (Vacuum Generators, U. K.) equipped with an unmonochromated Mg Kα X-ray source (1253.6 eV) and operating at 15 kV under a current of 20 mA. Samples were placed in an ultrahigh vacuum chamber (10^{-8} mbar) with electron collection by a hemispherical analyzer at a 90° angle. Signal decomposition was done using Spectrum NT, and the overall spectrum was shifted to ensure that the C−C/C−H contribution to the C 1s signal occurred at 285.0 kV. Comparison of the elementary surface composition was performed using

$$\frac{I_1/s_1}{I_2/s_2} \quad (5)$$

where I_i is the intensity of signal *i* (carbon, oxygen, or nitrogen) and s_i ($s_C = 0.00170$, $s_O = 0.00477$, and $s_N = 0{,}00299$) denotes the atomic sensitivity factor whose values were calculated from

$$s_i = \frac{T_i \lambda_i \sigma_i}{4\pi} \quad (6)$$

with T_i, λ_i, and σ_i being the transmission energy, the electron inelastic mean free path, and the photoionization cross-section for the X-ray source, respectively. T_i depends on the atomic kinetic energy E_i^{kin} (eV) according to

$$T_i = \frac{1}{(E_i^{kin})^{0.7}} \quad (7)$$

with $E_C^{kin} = 966.6$ eV, $E_O^{kin} = 722.6$ eV, and $E_N^{kin} = 851.6$ eV. The Penn algorithm[19] was used to calculate the electron inelastic mean free path λ_i ($\lambda_C = 2.63$ nm, $\lambda_O = 2.11$ nm, and $\lambda_N = 2.39$ nm), and σ_i values were taken from Scofield ($\sigma_C = 1$, $\sigma_O = 2.85$, and $\sigma_N = 1.77$).[20]

XPS was performed on the dried powder before and after surface modification.

Wide-angle X-ray diffraction data were recorded on dry starch powder at ambient temperature with a scattering angle step size of 0.02° between 4° and 30° on a Siemens D500 diffractometer equipped with a Cu Kα anode with $\lambda = 1.5406$ Å. X-ray diffraction analysis was performed on the dried powder before and after surface modification.

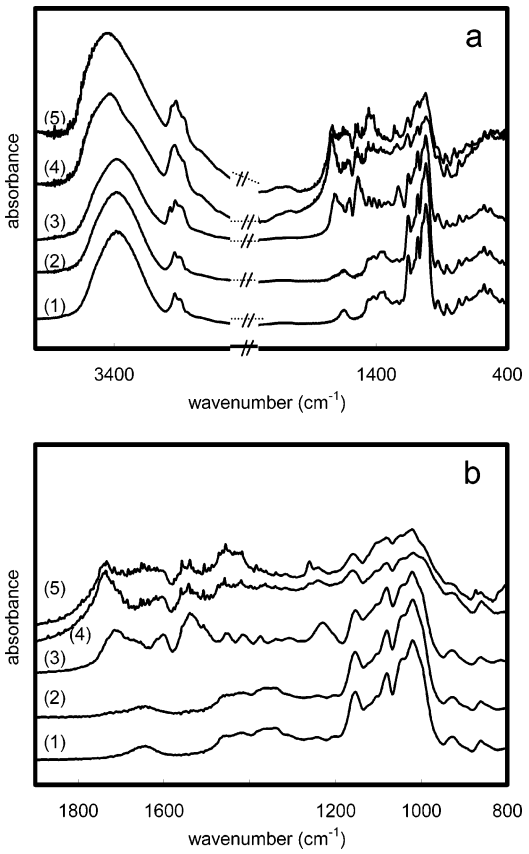

Figure 2. FTIR spectra of (1) unmodified and surface-grafted starch nanoplatelets with (2) PTHF1400, (3) PPGBE4000, (4) PCL10000, and (5) PCL42500. (b) View of FTIR spectra in the wavenumber range of 800−1900 cm^{-1}.

Results and Discussion

FTIR Spectroscopy. FTIR spectroscopy of the dry modified particles was obtained by inclusion in KBr pellets. Clear traces of modification can be noticed (Figure 2). Each of the modifications results in the following specific features:

(i) Three more or less distinct peaks around 2900 cm^{-1}, associated with the grafted alkyl chain (−CH_3, −CH_2−, and >CH− groups). The exact wavenumbers are 2954, 2918, and 2850 cm^{-1}, respectively.[21]

(ii) The appearance of a signal around 1700 cm^{-1} due to the appearance of urethane functions (−NHCOO−) for starch grafted with PPGBE, PTHF, and PCL and of ester functions (−COO−) for starch grafted with PCL. PCL-grafted starch shows a significant ester signal, as expected if grafting is successful.

In addition and as expected, the signal at 2250 cm^{-1} corresponding to the isocyanate functions disappears within 7 days of reaction time. No significant decrease in the signal around 3400 cm^{-1} was noticed although grafting should decrease the number of −OH functions. However, the large amount of

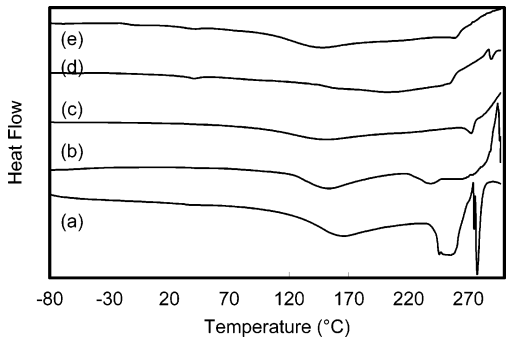

Figure 3. DSC traces of (a) ungrafted and (b) PTHF-, (c) PPGBE4000-, (d) PCL10000-, and (e) PCL42500-grafted starch nanocrystals. Positive values denote exothermicity, and traces are shifted vertically for sake of clarity.

Table 3. Melting (E_W^{melt}) Enthalpies and Weight Fractions of Starch ($\%_W^{starch}$) and Polymer ($\%_W^{polymer}$) Obtained from DSC Thermograms for Ungrafted and Grafted Starch Nanocrystals

	E_W^{melt} (J g^{-1})	$\%_W^{starch}$	$\%_W^{polymer}$ [a]
ungrafted	217.8	100	0
PTHF1400-grafted	183.3	84.2	15.8
PGBE4000-grafted	130.3	59.8	40.2
PCL10000-grafted	95.13	43.7	56.3
PCL42500-grafted	102.5	47.0	53.0

[a] $\%w^{polymer} = 1 - \%w^{starch}$.

internal and inaccessible hydroxyl groups relative to surface hydroxyl groups able to react, will absorb enough to limit the visibility of the signal's decrease. The grafting features are obvious for PPGBE4000-, PCL10000-, and PCL42500-grafted nanocrystals, but are more limited for PTHF1400-grafted nanoparticles.

Thermal Behavior. The thermal behavior of both ungrafted and grafted starch nanoparticles was characterized by DSC. Thermogram a in Figure 3 corresponds to ungrafted starch nanocrystals. A broad endothermic peak ranging between 110 and 180 °C was observed. It could be ascribed to starch melting in agreement with our previous study.[16] Endothermic events above 230 °C could represent not only the starch decomposition but also the thermally induced changes in the physical dimensions of the starch particles (meaning nonuniform contact of starch particles with the cell and so unpredictable heat-flow consumption). The thermograms obtained for grafted starch nanoparticles are shown in Figure 3 (thermograms b−e).

It is theoretically possible to deduce from DSC thermograms the weight fraction of both starch and grafted polymer by comparing the melting energies associated with grafted and ungrafted starch nanoparticles. However, the integration of the corresponding peak and its dissociation from any phenomenon associated with the grafted polymer layer are difficult to appraise so that the exact melting enthalpies of starch nanocrystals cannot be easily determined. As a consequence, the grafting efficiency deduced from DSC analysis is mainly qualitative but gives a good indication of the overall grafting efficiency nonetheless. The results are reported in Table 3. The starch weight content was obtained by dividing the total enthalpy associated with the melting process for the grafted nanoparticles by the corresponding enthalpy for the ungrafted nanoparticles. The weight fraction of grafted polymer was obtained from this value. From a qualitative point of view the grafting was efficient. Indeed, it was observed that the total enthalpy was systematically lower for grafted than for unmodified starch nanocrystals. This effect was more significant for PCL10000- and PCL42500-grafted starch, indicating a high grafting efficiency. Moreover, no crystallization of the grafted polymeric chains was reported because no specific melting endotherms were observed at the characteristic melting temperatures of the polymers. For stearic-acid-chloride-grafted starch nanocrystals, a distinct melting peak associated with the stearate surface phase was reported in a previous study.[16]

Also, the melting temperature for the grafted starch nanocrystals is lower compared to the ungrafted one and becomes lower with increasing polymer chain length. It could indicate that some disruption of the initial crystalline structure takes place. We will also see that the peaks in the wide-angle X-ray scattering patterns also become less defined.

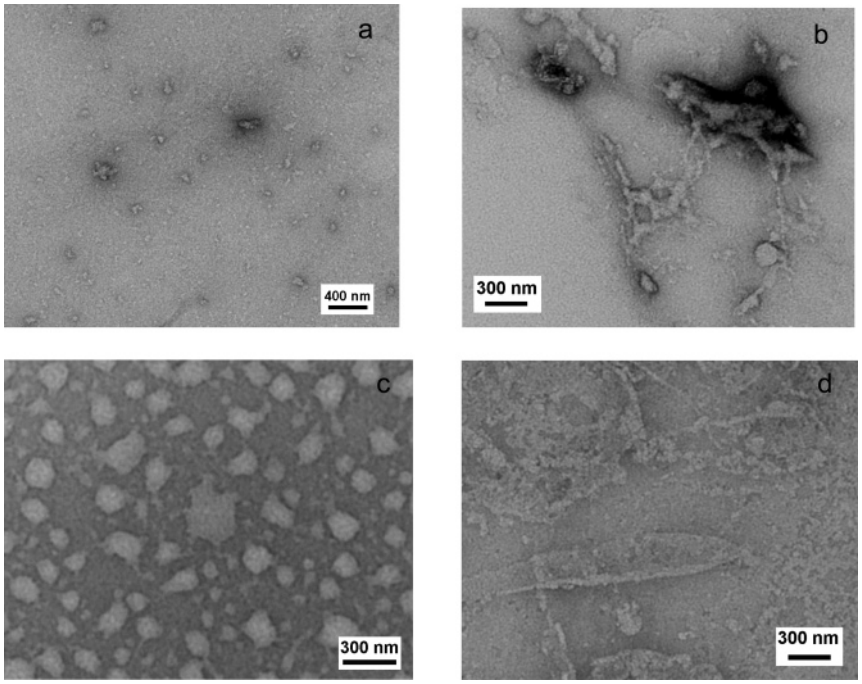

Figure 4. Transmission electron micrographs of (a) ungrafted, (b) PTHF1400-, (c) PPGBE4000-, and (d) PCL10000-grafted starch nanocrystals.

Transmission Electron Microscopy. TEM observations were performed for both unmodified and grafted starch nanocrystals. Figure 4a shows a transmission electron micrograph of unmodified nanoparticles. White dots surrounded by a gray halo correspond to individualized or barrets of several starch nanocrystals. In a previous study,[6] it was shown that crystalline residues obtained from acid hydrolysis of waxy maize starch granules consisted of platelet-like nanoparticles around 6−8 nm thick, 20−40 nm long, and 15−30 nm wide. They were found to occur as aggregates or barrets.

Figures 4b−d correspond to PTHF1400-, PPGBE4000-, and PCL10000-grafted starch nanoparticles, respectively. In Figure 4b, starch nanocrystals seem to be linked in larger aggregates. Threads linking starch nanoparticles are supposed to be composed of grafted PTHF chains. Figure 4c shows a transmission electron micrograph of PPGBE-grafted starch nanocrystals. The appearance of nanoparticles is completely different. They seem to be coated with a compact polymeric layer because their size increases compared to ungrafted particles. However, starch nanocrystal aggregates still remain individualized and fill the whole available space. The difference in aspect ratios between the two kinds of grafted nanoparticles could be possibly due to differences in affinity between grafted polymeric chains and the surface of the starch nanocrystal and the extent of grafting. PPGBE chains are expected to present a better affinity with starch than PTHF because of the higher density of oxygen atoms in the former. The consequence is a higher probability for grafted PPGBE chains to lie flat on the surface of the nanoparticle compared to PTHF chains. This will result in shielding of the starch nanocrystal surface, resulting in a reduction in interparticle hydrogen bonding. The attractive forces between PPGBE-grafted particles are then supposed to be lower than those for PTHF-grafted particles. In addition, FTIR spectroscopy showed a lower grafting efficiency for PTHF than for PPGBE, while the PPGBE chains are longer. Coverage of the starch surface by PPGBE and the consequential interparticle hydrogen-bonding blockage are thus expected to be more effective for PPGBE-grafted starch. This is clearly visible in these transmission electron micrographs. PCL-grafted nanocrystals (Figure 4d) seem to form a continuous film. It is the most cohesive material among those prepared.

Elemental Analysis. Elemental analysis was used to determine the efficiency of the polymer grafting. Indeed, from the knowledge of the elemental weight of both the glucose unit and the polymer used, it is possible to determine the theoretical elemental weight of the grafted glucose unit according to the number, x, of grafted polymeric chains. The corresponding formulas are reported in Table 4. From these formulas the evolution of the elemental weight composition of the polymer-grafted glucose unit can be plotted as a function of x, i.e., as a function of the grafting efficiency (Figure 5). Figures 5a−c correspond to the plots of the weight fractions of carbon, oxygen, and nitrogen, respectively, and Figures 5d and 5e correspond to the plots of the weight ratios of oxygen-to-carbon and nitrogen-to-carbon, respectively, versus x. Obviously, regardless of the grafted polymer and according to the chemical structure of the polymer, the theoretical weight fraction of nitrogen (%N) and carbon (%C) increases, while the theoretical weight fraction of oxygen (%O) decreases when increasing the grafting efficiency. Moreover, the theoretical weight ratio of oxygen-to-carbon (%O/%C) decreases, while the theoretical weight ratio of nitrogen-to-carbon (%N/%C) increases with the grafting efficiency.

By comparison of the theoretical and experimental data obtained for the elemental weight composition for ungrafted

Table 4. Theoretical Elemental Weight Compositions of Ungrafted and Grafted Starch Nanocrystals[a]

	%C	%N	%O	%N/%C	%O/%C
ungrafted	44.44	0	49.38	0	1.111
PTHF1400-grafted	$72 + 1104x/162 + 1679x \times 100$	$42x/162 + 1679x \times 100$	$80 + 368x/162 + 1679x \times 100$	$42x/72 + 1104x$	$80 + 368/72 + 1104x$
PGBE4000-grafted	$72 + 6528x/162 + 10343x \times 100$	$42x/162 + 10343x \times 100$	$80 + 2880x/162 + 10343x \times 100$	$42x/72 + 6528x$	$80 + 2880x/72 + 6528x$
PCL10000-grafted	$72 + 27048x/162 + 42833x \times 100$	$42x/162 + 42833x \times 100$	$80 + 12000x/162 + 42833x \times 100$	$42x/72 + 27048x$	$80 + 12000x/72 + 27048x$
PCL42500-grafted	$72 + 2604x/162 + 4192x \times 100$	$28x/162 + 4192x \times 100$	$80 + 1136x/162 + 4192x \times 100$	$28x/72 + 2604x$	$80 + 1136x/72 + 2604x$

[a] The variable x corresponds to the number of grafted polymeric chains per glucose unit.

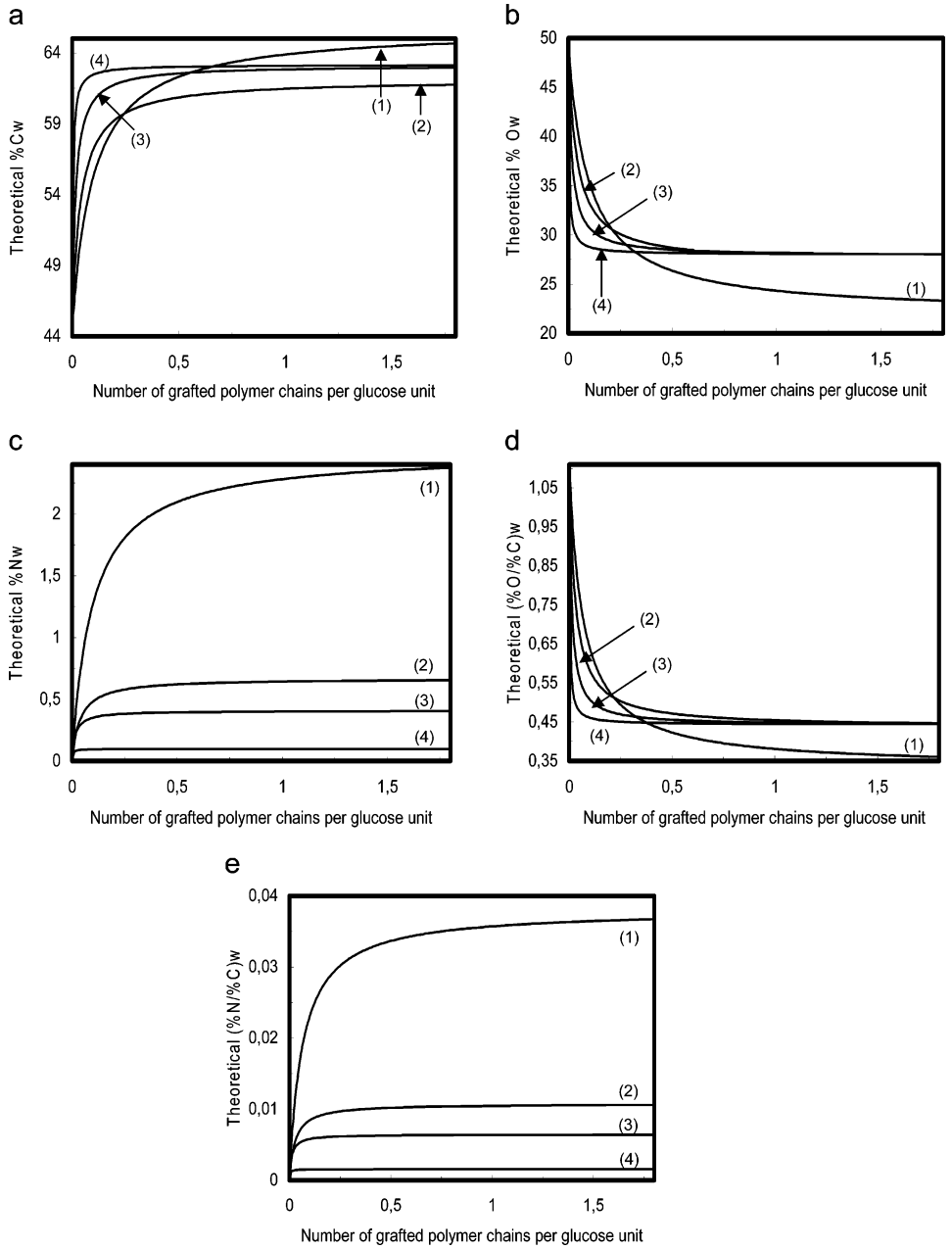

Figure 5. Evolution of the theoretical elemental weight fractions of (a) carbon, (b) oxygen, and (c) nitrogen and weight ratios of (d) oxygen-to-carbon and (e) nitrogen-to-carbon for (1) PTHF1400-, (2) PPGBE4000-, (3) PCL10000-, and (4) PCL42500-grafted starch nanocrystals versus the number of polymer chains grafted per glucose unit.

Table 5. Experimental and Corrected Elementary Weight Compositions for Ungrafted and Grafted Starch Nanocrystals[a]

	experimental values					corrected values		
	%C	%O	%N	%O/%C	%N/%C	%C	%O	%O/%C
ungrafted	41.20	51.71	<0.30	1.255	<0.007	44.44	49.38	1.111
PTHF1400-grafted	41.76	50.21	<0.30	1.202	<0.006	45.04	47.95	1.064
PGBE4000-grafted	49.91	39.21	3.70	0.786	0.074	53.83	37.44	0.696
PCL10000-grafted	49.65	42.21	1.31	0.850	0.026	53.55	40.31	0.752
PCL42500-grafted	48.37	41.49	6.83	0.858	0.141	52.17	39.62	0.760

[a] Experimental data correspond to values obtained directly from elemental analysis and corrected data account for the difference between experimental and corrected values for ungrafted starch nanocrystals.

starch, a good agreement was observed (Table 5). The theoretical and experimental values are 44.44% and 41.20%, 49.38% and 51.71%, and 1.111 and 1.255 for the elemental weight fractions of carbon and oxygen and weight ratio of oxygen-to-carbon, respectively. These differences can be possibly ascribed to both some impurities present in the sample and experimental error. In the following and to account for this difference, the experimental values refer to data obtained directly from elemental analysis, and the corrected values refer to the product between the experimental value obtained for a given material and the ratio of the corrected to experimental value for ungrafted starch nanocrystals. Both experimental and corrected elemental

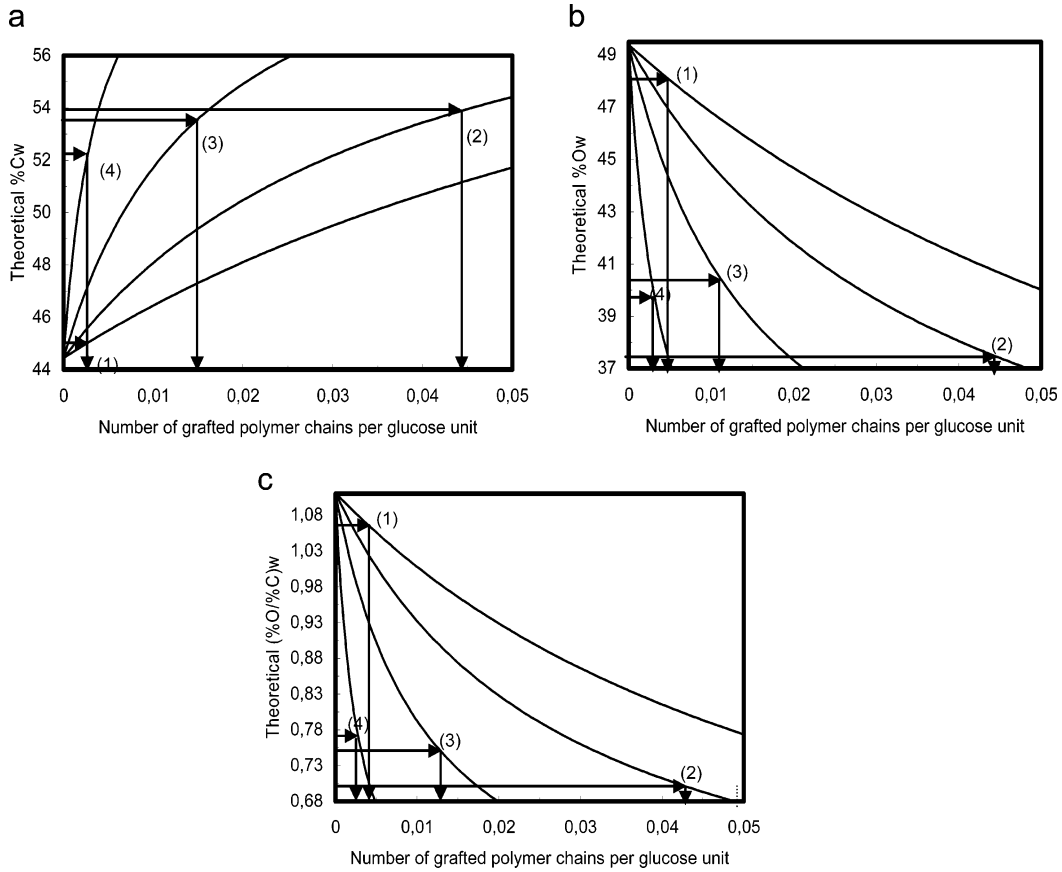

Figure 6. Graphical determination of the number of (1) PTHF1400, (2) PPGBE4000, (3) PCL10000, and (4) PCL42500 chains grafted per glucose unit from the weight fraction of (a) carbon and (b) oxygen and from the weight ratio of (c) oxygen-to-carbon.

weight composition data are reported in Table 5 for both ungrafted and grafted starch nanoparticles. From these corrected data, the number x of polymer chains grafted onto the starch nanoparticles can be determined for each material. Three methods can be used to determine the value of x via (i) the weight fraction of carbon (%C), (ii) the weight fraction of oxygen (%O), and (iii) the weight ratio of oxygen-to-carbon (%O/%C). Indeed, the weight fraction of nitrogen (%N) and the weight ratio of nitrogen-to-carbon (%N/%C) cannot be used because the nitrogen content is too low to give accurate results.

The three methods have been used, and the determination of the number x of polymer chains grafted onto the starch nanoparticles by each method is shown in Figure 6, which shows the evolution of the theoretical or corrected values as a function of x. The value of x for each material was determined from the knowledge of the corrected elemental weight composition. The results are collected in Table 6. The average value gives an estimate of the efficiency of the grafting while the standard deviation is representative of the reliability of the analysis. In Table 6, two sets of data are reported. The first one refers to the number of polymer chains grafted per glucose unit regardless of their localization in the starch nanocrystal, and the second one refers to the fraction of substituted hydroxyl groups among those that are able to react (the hydroxyl groups at the surface). The latter can be easily determined knowing that there are three hydroxyl groups per glucose unit and that only 20% of them are located at the surface and thus are able to react.[16] From Table 6, it is seen that the grafting of PPGBE4000 chains on starch nanocrystals was quite efficient because 7.27% of the hydroxyl groups from the surface have been substituted by the polymeric chain. The grafting of PCL10000 chains was moderately efficient with 2.19%, and the grafting of both PTHF1400 and PCL42500 chains displayed a much lower efficiency with only 0.68% and 0.51%, respectively, of OH groups able to react that actually reacted. Moreover, the standard deviation values show that elemental analysis was reliable to determine the efficiency of the grafting for PPGBE4000 and PCL42500 onto starch nanocrystals with variation factors of 2.64% and 7.83%, respectively. On the contrary, it was less reliable for PTHF1400- and PCL10000-grafted starch nanoparticles, with variation factors of 28.13% and 13.34%, respectively.

Table 6. Efficiency of the Grafting in Terms of the Number of Polymer Chains Grafted per Glucose Unit and Fraction of Hydroxyl Groups That Have Reacted among Those Accessible

	%C	%O	%O/%C	average
Number of Chains Grafted per Glucose Unit				
PTHF1400-grafted	0.0030	0.0053	0.0040	0.0041 ± 0.0012
PGBE4000-grafted	0.0430	0.0450	0.0430	0.0437 ± 0.0012
PCL10000-grafted	0.0150	0.0115	0.0130	0.0132 ± 0.0018
PCL42500-grafted	0.0028	0.0032	0.0032	0.0031 ± 0.0002
Fraction of Reacted OH Groups among Those Accessible				
PTHF1400-grafted	0.50	0.88	0.67	0.68 ± 0.19
PGBE4000-grafted	7.17	7.50	7.17	7.27 ± 0.19
PCL10000-grafted	2.50	1.92	2.17	2.19 ± 0.29
PCL42500-grafted	0.47	0.53	0.53	0.51 ± 0.04

Table 7 shows the weight fraction of both starch and polymer for grafted starch nanocrystals. These values were determined from the weight of each grafted polymer chain and from the number of chains per glucose unit. These data are in agreement with the values determined from DSC analysis.

X-ray Photoelectron Spectroscopy. X-ray photoelectron spectroscopy, like elemental analysis, provides a more quantitative measurement of the level of modification than DSC or FTIR

Table 7. Weight Fraction of Polymer and Starch for Grafted Starch Nanocrystals

	weight of a chain/unit	number of chains per glucose unit	starch content (wt %)	polymer content (wt %)
glucose unit	162	1	100	0
PTHF1400-grafted	1693	0.0041	95.89	4.11
PGBE4000-grafted	4174	0.0436	52.94	47.06
PCL10000-grafted	10293	0.0132	45.55	54.45
PCL42500-grafted	42793	0.0031	44.75	55.25

Table 8. Elemental Surface Compositions of Ungrafted and Grafted Starch Nanocrystals Determined from XPS Measurements

	%O	%N	%C	%O/%C	%N/%C
ungrafted	35.8	0.0	64.2	0.56	0.00
PTHF1400-grafted	29.7	2.2	68.1	0.44	0.03
PGBE4000-grafted	26.3	3.7	70.2	0.38	0.05
PCL10000-grafted	32.5	1.3	66.2	0.49	0.02
PCL42500-grafted	pastilles were not smooth enough to allow valid measurements				

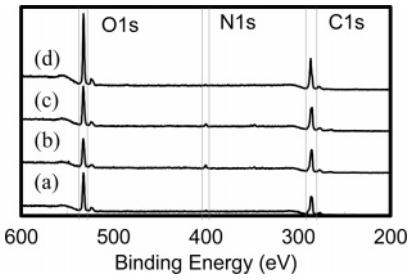

Figure 7. Global X-ray photoelectron spectra for (a) ungrafted and (b) PTHF1400-, (c) PPCBE4000- and (d) PCL10000-grafted starch nanocrystals with signal assignments.

spectroscopy. This tool is appropriate to study the chemical changes resulting from the surface modifications, as its maximum investigation thickness is about 10 nm. The full X-ray photoelectron spectra for both ungrafted and grafted starch nanocrystals are shown in Figure 7. The signals observed around binding energies of 531, 402, and 287 eV correspond to the 1s orbital electrons of oxygen, nitrogen, and carbon, respectively. The elemental surface compositions as well as the ratios of oxygen-to-carbon and nitrogen-to-carbon of the different samples are given in Table 8. The ratio of oxygen-to-carbon for ungrafted starch nanoparticles is 0.56 while the expected value was 0.83. This is an indication, as already reported in previous studies, that unmodified starch nanocrystals are not only composed of polysaccharides but also contain hydrocarbon impurities that tend to increase the carbon content.[15,16,22] However, the nitrogen content is found to be negligible, in contradiction with previous studies that reported the presence of proteins.[15,23] For grafted nanoparticles, the increase of both the nitrogen and carbon contents compared to ungrafted nanocrystals shows that the grafting was quite efficient. The decomposition of the main carbon signals (Table 9 and Figure 8) leads to the following conclusions when comparing grafted to ungrafted nanoparticles:

- The C−C/C−H contribution (C1) increases while the C−O contribution (C3) decreases. It is ascribed to the fact that the grafted polymeric chains contain more alkyl groups than ether functions (when compared to the original starch particles).
- The C−N linkages appear (contribution C2), confirming the surface grafting of each of the polymer using 2,4-TDI.
- The O−C−O/C═O contribution (C4) decreases. Indeed, starch is mainly responsible for this signal, and its occurrence decreases as long polymeric chains, which contain less of this functionality, are grafted.
- The O−C═O contribution (C5) increases significantly for starch nanocrystals grafted with PCL because this polymer is a polyester.

All of these evolutions in the decomposition of the main carbon signal give additional evidence of the efficiency of the grafting of starch nanoparticles with polymeric chains. The exact number of chains grafted onto the surface of the nanocrystals is difficult to know due to the depth of XPS analysis. However, it is in qualitative agreement with our previous results.

No XPS analysis was performed for PCL42500-grafted starch nanocrystals because the surface of this sample was not smooth enough.

Wide-Angle X-ray Diffraction. X-ray diffraction measurements were performed for both ungrafted and grafted starch nanocrystals to verify if any alteration of their crystallinity occurred upon chemical surface modification. X-ray diffraction powder patterns are displayed in Figure 9. Ungrafted waxy maize starch nanoparticles (Figure 9a) show a scattering pattern similar to the one generally obtained for the A-type, characteristic of cereal starches, with main peaks at $2\theta = 18°$ ($d = 0.49$ nm), $2\theta = 17.2°$ ($d = 0.52$ nm), $2\theta = 15.5°$ ($d = 0.57$ nm), and $2\theta = 23°$ ($d = 0.39$ nm).[24−28]

After surface modification with PTHF1400, PPGBE4000, PCL10000, and PCL42500, it is observed that the crystalline structure of starch nanocrystals is kept intact although the diffraction peaks are less well-defined due to the formation of a polymer layer at the surface of the nanoparticles. For PTHF1400-grafted nanocrystals (Figure 9b) a broad halo centered around $2\theta = 5.75°$ ($d = 1.54$ nm) appears. In addition, an ill-defined shoulder is observed on the low scattering angle side of the peak at $2\theta = 15.5°$ ($d = 0.57$ nm) for each of the modified starch particles, resulting in a broadening of this diffraction peak. These phenomena can be attributed to the coating of starch nanoparticles with a grafted polymeric layer, which provides a diffusing layer around the nanoparticles. The spectra also show that there is no crystallization of the grafted polymer chains, as no distinct additional diffraction signals emerge.

Contact Angle Measurements. Figure 10 shows the dynamic behavior of the contact angle for a drop of distilled water deposited onto the surface of both ungrafted and PTHF1400- and PPGBE-4000-grafted starch nanocrystals. A clear and significant increase of the contact angle with water is observed after grafting, which shows that, while ungrafted starch was completely hydrophilic, it becomes more hydrophobic after grafting. The initial contact angle value is about twice that of ungrafted nanocrystals after grafting PPGBE4000. It is ascribed to the coverage of starch nanoparticles with a hydrophobic polymeric layer. In addition, for ungrafted starch nanoparticles, the contact angle value decreases with time, whereas it remains remarkably constant for modified substrates. It was verified that the spreading phenomenon was due to spreading of the drop rather than penetration by capillarity because of the porous character of the pellets prepared for these measurements.

Contact angle values for each tested liquid are collected in Table 10 for ungrafted and PTHF1400- and PPGBE4000-grafted nanoparticles. PCL-grafted starch nanocrystals were not tested because the surfaces of the samples were not smooth enough. The contact angle values reported correspond to the equilibrium contact angles found at longer times (e.g., Figure 10 for contact angle with water). This guarantees the absence of drop deposit

Table 9. Surface Functional Group Composition Obtained from the Decomposition of the C 1s Signal with Average Binding Energy Position

	C1 C−C, C−H	C2 C−N	C3 C−O	C4 O−C−O, C=O	C5 O−C=O
binding energy (eV)	285.00	286.20	286.50	288.05	289.00
ungrafted	25.0%	0.0%	58.2%	14.9%	1.9%
PTHF1400-grafted	46.2%	4.5%	38.4%	7.9%	3.0%
PGBE4000-grafted	55.0%	6.5%	29.8%	6.5%	2.2%
PCL10000-grafted	43.7%	1.5%	40.1%	7.2%	7.5%

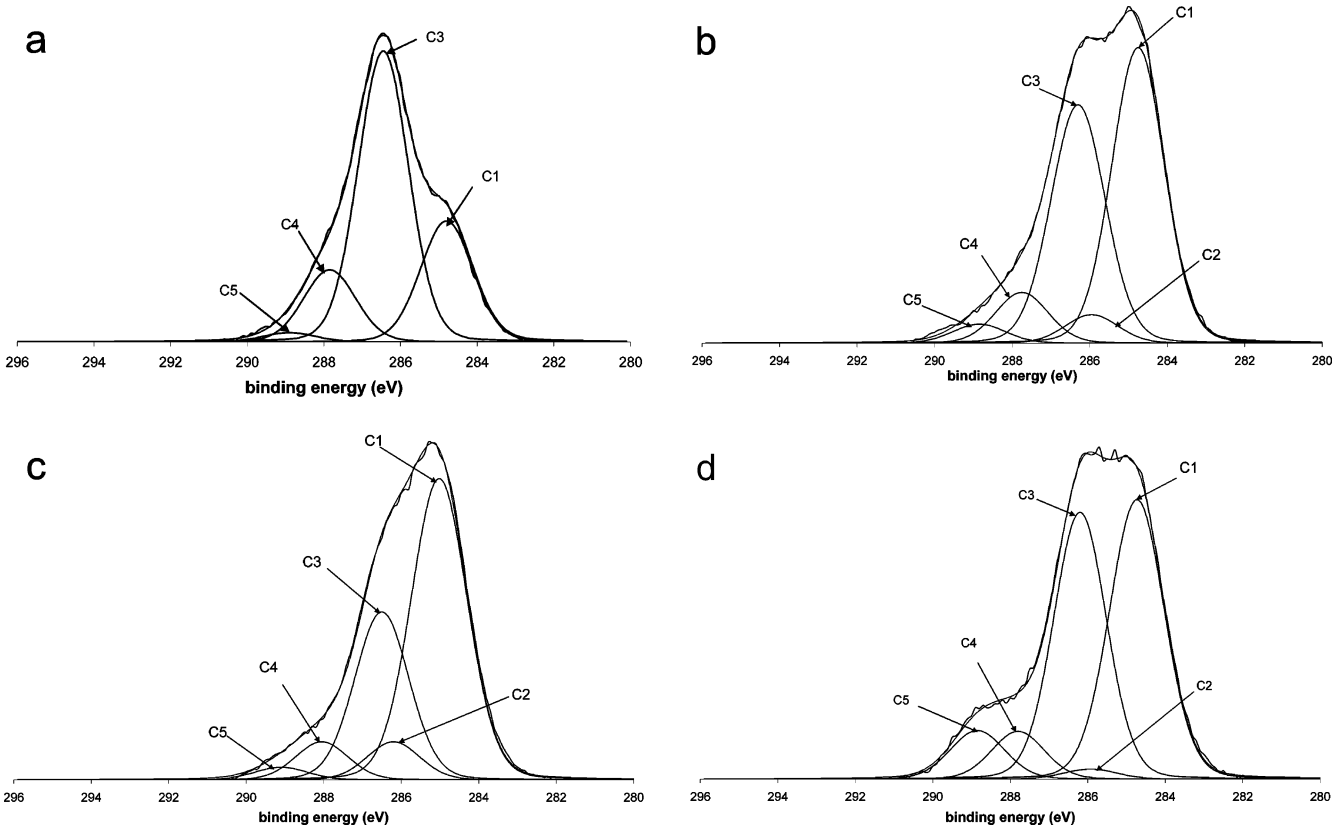

Figure 8. Decomposition of the C 1s signal into its constituent contributions for (a) ungrafted and (b) PTHF1400-, (c) PPGBE4000-, and (d) PCL10000-grafted starch nanocrystals.

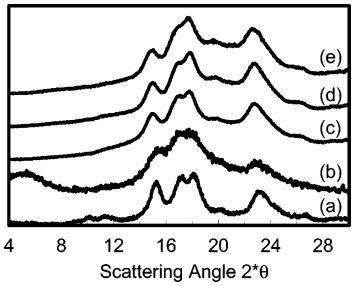

Figure 9. X-ray diffraction patterns for (a) ungrafted and (b) PTHF1400-, (c) PPGBE4000-, (d) PCL10000-, and (e) PCL42500-grafted starch nanocrystals.

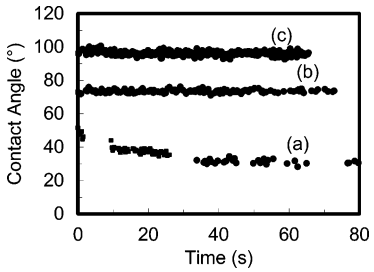

Figure 10. Water contact angle versus time for (a) ungrafted and (b) PTHF1400- and (c) PPGBE4000-grafted starch nanocrystals.

and initial spreading effects. Indeed, the volume of the drop was followed, and its constancy guarantees that no penetration occurred.

By plotting eq 3 (Figure 11), the polar, γ^p, dispersive, γ^d, and total, γ, surface energy were determined for each substrate. Results are reported in Table 11. Data obtained for ungrafted starch nanocrystals agree with previous observations.[15] It is observed that the polar contribution to the surface energy is dramatically reduced after polymer chains were grafted onto the surface of starch nanoparticles, especially for PPGBE4000. This phenomenon is ascribed to the fact that the polymer chains grafted onto starch nanocrystals display a significantly less polar character than starch. In addition, the total surface energy for PTHF- and PPGBE-grafted starch nanoparticles is close to those found in the literature for the polymers by themselves.[29] This is additional evidence that modified nanocrystals are covered by a polymeric layer. Coupled with the relatively low grafting efficiencies determined earlier, it can thus be derived that the grafted polymer chains lay flat onto the starch surface to provide complete coverage with minimal grafting. This conformation is believed to be due to attraction between the unreacted surface hydroxyl groups and the oxygen in the polymer backbone. This

Table 10. Contact Angle Values of the Tested Liquids for Ungrafted and Grafted Starch Nanocrystals

	water	formamide	diiodomethane
ungrafted	32.6	20.5	33.0
PTHF1400-grafted	81.2	56.7	43.5
PGBE4000-grafted	96.9	66.3	40.8
PCL10000-grafted	pastilles were not smooth enough		
PCL42500-grafted	to allow valid measurements		

Table 11. Surface Energy Contributions for Ungrafted and Grafted Starch Nanocrystals

	γ_S^p (mN m^{-1})	γ_S^d (mN m^{-1})	γ_S (mN m^{-1})
ungrafted	32.71	29.59	62.30
PTHF1400-grafted	4.12	34.22	38.34
PGBE4000-grafted	0.14	39.19	39.33

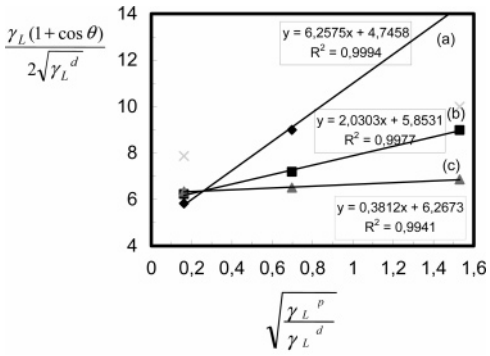

Figure 11. Graphical determination of the surface energy for (a) ungrafted and (b) PTHF1400- and (c) PPGBE4000-grafted starch nanocrystals. Inset correspond to the linear regressions of each set of data.

has also been seen for starch nanocrystals modified with poly(ethylene glycol).[16]

Conclusions

The surfaces of starch nanocrystals prepared by acid hydrolysis of waxy maize starch granules were chemically modified using four polymers, namely, poly(tetrahydrofuran) (M_n = 1400 g mol^{-1}), poly(propylene glycol) monobutyl ether (M_n = 4000 g mol^{-1}), and poly(caprolactone) (M_n = 10 000 g mol^{-1} and M_n = 42 500 g mol^{-1}). The evidence of the occurrence of grafting of the polymers was checked by FTIR and X-ray photoelectron spectroscopies, DSC analysis, and contact angle measurements. It was verified by X-ray diffraction that the initial crystalline structure of the nanoparticles was preserved. Contact angle measurements showed that the surface chemical modification with isocyanate or anhydride functions allowed enhancement of the nonpolar nature of original starch nanocrystals. Possible applications of these materials include packaging and composites. Indeed, these co-continuous materials can be hot-pressed, and if cohesive enough, the resulting films can be mechanically tested. Results will be reported in a forthcoming publication. PCL-grafted starch nanoparticles could possibly be used in biomedical applications.

Acknowledgment. Financial support for this work was provided by ADEME (Agence Française de l'Environnement et de la Maîtrise de l'Energie, convention 0401C0011). We thank Isabelle Paintrand (CERMAV) for her help with the TEM imaging of the starch nanocrystals, Grégory Berthomé (LTPCM-ENSEEG) for his help with the XPS experiments, Hervé Roussel and Stéphane Coindeau (CMTC-ENSEEG) for their help with X-ray diffraction, the laboratory SAC of the Centre National de la Recherche Scientifique for the elementary analyses, and Roquette S.A. (Lestrem, France) for supplying the waxy maize starch. W.T. also thanks the European Commission for its financial support through his Marie Curie Intra-European Fellowship (MEIF-CT-2005-025125).

References and Notes

(1) Davis, G.; Song, J. H. *Ind. Crops Prod.* **2006**, *23* (2), 147−161.
(2) Azizi Samir, M. A. S.; Alloin, F.; Dufresne, A. *Biomacromolecules* **2005**, *6* (2), 612−626.
(3) Dufresne, A. *J. Nanosci. Nanotechnol.* **2006**, *6* (2), 322−330.
(4) Naëgeli, C. W. *Ann. Chem.* **1874**, *173*, 218−227.
(5) Lintner, C. J. *J. Prakt. Chem.* **1886**, *34*, 378−386.
(6) Putaux, J. L.; Molina-Boisseau, S.; Momaur, T.; Dufresne, A. *Biomacromolecules* **2003**, *4* (5), 1198−1202.
(7) Angellier, H.; Choisnard, L.; Molina-Boisseau, S.; Ozil, P.; Dufresne, A. *Biomacromolecules* **2004**, *5* (4), 1545−1551.
(8) Dufresne, A.; Cavaillé, J. Y.; Helbert, W. *Macromolecules* **1996**, *29* (23), 7624−7626.
(9) Dufresne, A.; Cavaillé, J. Y. *J. Polym. Sci., Part B: Polym. Phys.* **1998**, *36* (12), 2211−2224.
(10) Angellier, H.; Molina-Boisseau, S.; Lebrun, L.; Dufresne, A. *Macromolecules* **2005**, *38* (9), 3783−3792.
(11) Angellier, H.; Molina-Boisseau, S.; Dufresne, A. *Macromolecules* **2005**, *38* (22), 9161−9170.
(12) Angellier, H.; Molina-Boisseau, S.; Dufresne, A. *Macromol. Symp.* **2006**, *233* (1), 132−136.
(13) Angellier, H.; Molina-Boisseau, S.; Dole, P.; Dufresne, A. *Biomacromolecules* **2006**, *7* (2), 531−539.
(14) Kristo, E.; Biliaderis, C. G. *Carbohydr. Polym.* **2007**, *68* (1), 146−158.
(15) Angellier, H.; Molina-Boisseau, S.; Belgacem, M. N.; Dufresne, A. *Langmuir* **2005**, *21* (6), 2425−2433.
(16) Thielemans, W.; Belgacem, M. N.; Dufresne, A. *Langmuir* **2006**, *22* (10), 4804−4910.
(17) Belgacem, M. N.; Quillerou, J.; Gandini, A. *Eur. Polym. J.* **1993**, *29* (9), 1217−1224.
(18) Adamson, A. W. *Physical Chemistry of Surfaces*, 5th ed.; Wiley: New York, 1990.
(19) Tanuma, S.; Powell, C. J.; Penn, D. R. *Surf. Sci.* **1987**, *192* (1), L849−L857.
(20) Scofield, J. H. *J. Electron Spectrosc. Relat. Phenom.* **1976**, *8* (2), 129−137.
(21) RIO-DB Spectral Database for Organic Compounds, 2006. http://riodb.ibase.go.jp/sdbs/.
(22) Varma, A. *J. Carbohydr. Polym.* **1984**, *4* (6), 473−480.
(23) Rindlav-Westling, A.; Gatenholm, P. *Biomacromolecules* **2003**, *4* (1), 166−172.
(24) Zobel, H. F. *Starch/Staerke* **1988**, *40* (1), 1−7.
(25) Matveev, Y. I.; van Soest, J. J. G.; Nieman, C.; Wasserman, L. A.; Protservo, V. A.; Ezernitskaja, M.; Yuryev, V. P. *Carbohydr. Polym.* **2001**, *44* (2), 151−160.
(26) Katopo, H.; Song, Y.; Jane, J.-L. *Carbohydr. Polym.* **2002**, *47* (3), 233−244.
(27) Buléon, A.; Gérard, C.; Riekel, C.; Vuong, R.; Chanzy, H. *Macromolecules* **1998**, *31* (19), 6605−6610.
(28) Van Soest, J. J. G.; Hulleman, S. H. D.; de Wit, D.; Vliegenthart, J. F. G. *Ind. Crops Prod.* **1996**, *5* (1), 11−22.
(29) *Polymer Handbook*, 4th ed.; Brandrup, J.; Immergut, E. H., Grulke, E. A., Abe, A., Bloch, D. R., Eds.; Wiley: New York, 2003; Vol. 2.

BM700468F